IFN-γ producing CD4+ T cells promote experimental cerebral malaria by modulating CD8+ T cell accumulation within the brain

Ana Villegas-Mendez[*],[§],[1], **Rachel Greig**[*],[¶],[1], **Tovah N. Shaw**[*],[§], **J. Brian de Souza**[*],[†], **Emily Gwyer Findlay**[*],[□], **Jason S. Stumhofer**[‡],[#], **Julius C. R. Hafalla**[*], **Daniel G. Blount**[*],[††], **Christopher A. Hunter**[‡], **Eleanor M. Riley**[*], and **Kevin N. Couper**[*],[§]

[*]Department of Immunology and Infection, Faculty of Infectious and Tropical Diseases, London School of Hygiene and Tropical Medicine, Keppel Street, London WC1E 7HT, UK.

[†]Department of Immunology and Molecular Pathology, University College London Medical School, 46 Cleveland Street, London, W1T 4JF, UK

[‡]Department of Pathobiology, University of Pennsylvania, 380 South University Ave, Philadelphia, PA 19104, USA

Abstract

It is well established that IFN-γ is required for the development of experimental cerebral malaria (ECM) during *Plasmodium berghei* ANKA infection of C57BL/6 mice. To date, however, the temporal and tissue-specific cellular sources of IFN-γ during *P. berghei* ANKA infection have not been investigated and it is not known if IFN-γ production by a single cell type in isolation can induce cerebral pathology. In this study, using IFN-γ reporter mice, we show that NK cells dominate the IFN-γ response during the early stages of infection in the brain, but not in the spleen, before being replaced by CD4+ and CD8+ T cells. Importantly, we demonstrate that IFN-γ producing CD4+ T cells, but not innate or CD8+ T cells, can promote the development of ECM in normally resistant IFN-γ$^{-/-}$ mice infected with *P. berghei* ANKA. Adoptively transferred wild-type (WT) CD4+ T cells accumulate within the spleen, lung and brain of IFN-γ$^{-/-}$ mice and induce ECM through active IFN-γ secretion, which increases accumulation of endogenous IFN-γ$^{-/-}$ CD8+ T cells within the brain. Depletion of endogenous IFN-γ$^{-/-}$ CD8+ T cells abrogated the ability of WT CD4+ T cells to promote ECM. Finally we show that IFN-γ production specifically by CD4+ T cells is sufficient to induce expression of CXCL9 and CXCL10 within the brain, providing a mechanistic basis for the enhanced CD8+ T cell accumulation. These observations demonstrate, for the first time, the importance of and pathways by which IFN-γ-producing CD4+ T cells promote the development of ECM during *P. berghei* ANKA infection.

Introduction

Plasmodium berghei ANKA infection in susceptible strains of mice results in the development of experimental cerebral malaria (ECM), a fatal neuropathology characterised by sequestration of parasite infected red blood cells (iRBC) and leukocytes within the brain

Corresponding author: kevin.couper@manchester.ac.uk Tel: (44) 0161 275 1743.
[§]Present address: Faculty of Life Sciences, University of Manchester, A V Hill Building, Oxford Road, M13 9PT, UK
[¶]Present address: Breakthrough Breast Cancer, Weston House, 246 High Holborn, London WC1V 7EX
[□]Present address: MRC Centre for Inflammation Research, Queen's Medical Research Institute, University of Edinburgh, Scotland, UK
[#]Present address: Department of Microbiology and Immunology, University of Arkansas for Medical Sciences, 4301 W. Markham St, Little Rock, AR, 72205, USA
[††]Present address: Oxford Biomedica (UK) Ltd, Robert Robinson Avenue, Oxford, OX4 4GA, UK
[1]These authors contributed equally to the work.

(reviewed 1-3). The clinical signs of ECM, including ataxia, paralysis, coma and ultimately death, are analogous to those of human cerebral malaria and - as in human disease (reviewed 1) - although treatment with anti-malarial drugs can prevent mortality associated with ECM, surviving mice may display long-lasting neurological deficits, including impaired memory (4, 5).

IFN-γ dependent processes are involved in the development of cerebral pathology during *P. berghei* ANKA infection, as evidenced by the complete resistance to ECM of IFN-$\gamma^{-/-}$ and IFN-γR$^{-/-}$ mice on normally susceptible backgrounds (6, 7). Interferon signalling pathways are significantly upregulated within the brains of ECM-susceptible mice during infection with *P. berghei* ANKA, suggesting that IFN-γ may directly influence the local cerebral environment (8, 9). In support of this hypothesis, IFN-γ has been shown to promote macrophage accumulation and macrophage effector functions in the brain during infection (6), and to direct migration of CD8$^+$ T cells into the brain through CXCL9 and CXCL10 dependent pathways (7, 10-13). Although the functional role of brain-accumulating macrophages/monocytes in promoting ECM is unclear (14, 15), it is well established that T cells contribute to the initiation and/or terminal development of cerebral pathology (1, 3, 14). IFN-γ also promotes the upregulation of adhesion molecules on brain endothelial cells during infection, potentially enhancing iRBC and leukocyte sequestration within the brain vasculature and transmigration of cells into the perivascular space. (6, 10). Indeed, it has recently been shown that iRBC and leukocyte accumulation is reduced in the brains of IFN-$\gamma^{-/-}$ mice during infection (15, 16)

IFN-γ can be produced by various cell populations during malaria infection, including NK cells, NK T cells, $\gamma\delta$ TCR$^+$ T cells and $\alpha\beta$ TCR$^+$ CD4$^+$ and CD8$^+$ T cells (reviewed 17, 18). Strikingly, and consistent with the notion of temporal activation of innate and adaptive immune responses, sequential production of IFN-γ by NK cells and CD4$^+$ T cells has been shown to occur *in vitro* following exposure of PBMCs to *P. falciparum* parasites (19). In some malaria infections, IFN-γ production by CD4$^+$ T cells may be transient due to changes in the immunological environment. For example, during *P. chabaudi* AS and *P. yoelii* infections changes in the DC compartment in the later stages of infection result in reduced IFN-γ production by CD4$^+$ T cells concomitant with upregulation of IL-4 and IL-10 production (20, 21). With specific relevance to *P. berghei* infection, an early burst of IFN-γ during the early stages of infection has been associated with protection against ECM (22). Although there are many potential cellular sources of IFN-γ during *P. berghei* ANKA infection, it is currently unclear whether IFN-γ production by an individual cell population in a specific tissue location governs the development of ECM or whether sequential or concomitant induction of IFN-γ by different cell types and in different locations is required.

Although ECM is referred to as a classical IFN-γ-mediated condition, it has been shown that IFN-γ-producing CD4$^+$ T cells are essential for the migration and recruitment of Th17 cells into the CNS during experimental autoimmune encephalomyelitis (EAE) (23) and that Th17 cells, rather than IFN-γ-producing cells, are responsible for much of the pathology of EAE (24, 25). Thus, it is possible that IL-17 may mediate the development of ECM during *P. berghei* ANKA infection downstream of IFN-γ production. IL-17 can exert a number of direct effects in the CNS that may contribute to neuropathology during malaria infection, including direct neuronal damage (26), disruption of the blood brain barrier (27) and activation of astrocytes (28, 29). To date, the role of IL-17 during *P. berghei* ANKA infection has not been examined in detail.

In this study we have ruled out any role for IL-17 in the development of ECM and have used IFN-γ reporter mice (30) to examine the dynamics of IFN-γ production within distinct anatomical locations during *P. berghei* ANKA infection. We have subsequently calculated

the contribution of IFN-γ production by each distinct cell type to the total IFN-γ response. Despite the myriad of cells that can produce IFN-γ during infection, using an adoptive transfer model, we show that IFN-γ production specifically by CD4^{+} T cells, and not by innate cells or CD8^{+} T cells, can promote signs of ECM in normally resistant infected IFN-γ^{−/−} mice. Finally, we provide mechanistic evidence that IFN-γ production exclusively by CD4^{+} T cells causes ECM by increasing CD8^{+} T cell migration and accumulation within the brain, potentially via the local upregulation of CXCL9 and CXCL10 within the brain. Our results significantly extend our understanding of the pathogenesis of ECM during *P. berghei* ANKA infection.

Materials and Methods

Animals and parasites

C57BL/6N (WT), C57BL/6 IFN-γ knock out (IFN-γ^{−/−}), C57BL/6 RAG-1 knock out (RAG-1^{−/−}) and C57BL/6 Ly5.1 (Ly5.1[+]) mice were bred in-house at London School of Hygiene and Tropical Medicine, UK, or purchased from Harlan, Oxford, UK. C57BL/6 IFN-γ reporter mice (YETI: 30) were kindly provided by Dr Mohrs, Trudeau Institute and were bred at Harlan, UK. Animals were maintained in individual ventilated cages. C57BL/6 IL-17 receptor knock out (IL-17R^{−/−}) mice, provided by Amgen, Inc. USA, which are deficient in IL-17A and IL-17F responses, were bred and maintained at Department of Pathobiology at the University of Pennsylvania, Philadelphia, PA, USA. C57BL/6J mice used as controls in IL-17R^{−/−} experiments were purchased from Jackson Laboratories (Bar Harbor, ME, USA) and were maintained at the University of Pennsylvania. Male and female mice were used in separate experiments between 6 and 10 weeks of age.

Cryopreserved *P. berghei* ANKA parasites, derived from the *Pb*A clone 15cy1, were thawed and passaged once in vivo before being used to infect experimental animals. Experimental mice were infected intravenously (i.v.) with 10^4 parasitised red blood cells. In some experiments mice were injected i.p. with 250 μg of anti-CD8 (53-7.62) or anti-IFN-γ (XMG1.2) on days −2, 0, 2, 4 and 6 of infection. Isotype control antibodies (rat IgG2a and rat igG1 respectively) were used to verify the specific activity of anti-IFN-γ and anti-CD8 antibodies administered in vivo. All antibodies were obtained from BioXcell ltd (New Hampshire, USA). Parasitaemia was monitored daily by microscopical examination of Giemsa (BDH) stained thin blood smears. Signs of disease were classified using the following clinical scale: 1=no signs; 2=ruffled fur/and or abnormal posture; 3=lethargy; 4=reduced responsiveness to stimulation and/or ataxia and/or respiratory distress/ hyperventilation; 5=prostration and/or paralysis and/or convulsions. All animals were immediately euthanized when observed at stage 4 or 5. Stages 2-3 were classified as prodromal signs of ECM and stages 4-5 were classified as ECM. Animals in stages 4 and 5 of infection invariably showed signs of cerebral pathology, including blocked vessels, haemorrhages, odema, perivascular cuffing and disruption and damage to cerebral vasculature endothelial linings following histological examination.

Flow cytometry

Splenic single cell suspensions were prepared by homogenisation through a 70 μm cell strainer (BD Bioscience). Brains were chopped into small pieces and incubated in HBSS containing 10% FCS with collagenase/dispase (final concentration 2 mg/ml) (Sigma) for 45mins at room temperature. The suspension was filtered through a 70 μm cell strainer before being overlayed on a 30% percoll gradient and centrifuged at $1800 \times g$ for 10 minutes. The pellet was collected and the supernatant was discarded. Spleen and brain samples were treated with RBC lysing buffer (BD Pharmingen) to remove RBC, washed and resuspended in flow cytometry buffer (HBSS with 2% FCS). Absolute cell numbers were

calculated using a haemocytometer and live/dead cell differentiation was performed using Trypan Blue (Sigma). To examine T cell activation, 1×10^6 cells per sample were surface stained with anti-mouse CD4 (RM4.4), anti-mouse CD8 (53-6.7), anti-mouse CD44 (IM7), anti-mouse CD62L (MEL-14), anti-mouse CD69 (H1. 2F3), anti-mouse CD71 (R17217), anti-mouse CD27 (LG.7F9), anti-mouse KLRG-1 (2F1), anti-mouse CD25 (PC61), anti-mouse CCR5 (HM-CCR5), anti-mouse CXCR3 (CXCR3-173) and anti-mouse CD45.1 (A20) or permeabilised (0.1% Saponin/PBS) and stained with anti-mouse Granzyme B (NGZB). NK and NK T cells were identified by staining with anti-mouse CD3 (145-2C11) and anti-mouse CD49b (DX5). To assess intracellular cytokine production, 1×10^6 live cells were incubated with PMA (200 ng/ml) and ionomycin (1 μg/ml) in the presence of Brefeldin A (1:1000) for 5hrs at 37°C 5% CO_2. The cells were washed and stained after permeabilising cells with anti-mouse IFN-γ (XMG1.2) and anti-mouse TNF (MP6-XT22). All antibodies were obtained from eBioscience or BD Biosciences. Fluorescence minus one (FMO) controls and isotype control antibodies were used to validate flow cytometric results. Flow cytometric acquisition was performed using a FACSCalibur (BD Immunocytometry Systems, USA), LSR II (BD Immunocytometry Systems, USA) or Miltenyi MACSQuant (Miltenyi, Inc) and all analysis was performed using Flowjo software (Treestar Inc., OR, USA).

Determination of cerebral pathology

To examine the status (permeability) of the blood brain barrier, mice were injected i.v. with 200 μl of 1% Evans blue (Sigma Aldrich, UK). After one hour, mice were sacrificed and the brains were removed following whole-body perfusion with 15 ml of PBS. In separate experiments, brains were removed from mice (following perfusion) that were not injected with Evans blue and placed in 10% formol saline. Preserved samples were then sectioned and stained with Hamatoxylin and Eosin (H & E) (Independent Histopatholgy Services, 100a New Cavendish Street, London, UK). The presence of haemorrhages, inflamed and damaged blood vessels (including occluded vessels) and perivascular cuffing was then examined by microscopy.

Real-time PCR

RNA isolation from brains was performed using RNeasy isolation kits according to the manufacturer's instructions (Qiagen). Isolated RNA was DNAse treated to remove genomic DNA prior to synthesis of cDNA. cDNA expression for each sample was standardised using the housekeeping gene β-actin. Validated Taqman gene expression assays for β-actin, CXCL9, CXCL10, VCAM-1 and ICAM-1 were purchased from ABI Biosystems (Warrington, UK). PCR Cycling (Taqman, ABI 7500 fast RT-PCR) conditions were: 50 °C for 2 min, 95 °C for 10 min followed by 40 cycles of 15 sec at 95 °C completed with 1 min at 60 °C. Parasite levels were determined by Syber green PCR using *P. berghei* 18s and *P. berghei* carbamoyl phosphate synthetase DNA primers, normalised to mouse β-actin or tyrosine 3-monooxygenase activation protein (YWHAZ), respectively. *P. berghei* 18s primers: 5′-AAGCATTAAATAAAGCGAATACATCCTTAC-3′ and 5′-GGAGATTGGTTTTGACGTTTATGTG-3′; β-actin primers: 5′-GTGGGCCGCTCTAGGCACCAA-3′ and 5′-CTCTTTGATGTCACGCACGATTTC-3′; Carbamoyl phosphate synthetase primers 5′-TGGAATGTGTGAACATGATAAATA-3′ and 5′-TTTCCTGGCCCATTTGATAA-3′; YWHAZ primers: 5′-TTCTATTCCTCTATTTCCATGTTGG-3′ and 5′-AGGAGGAGGAGGAAGAGGAG-3′. All PCR data are presented as fold change ($\log_{10}$) in gene expression in brains from infected IFN-γ$^{-/-}$ mice that received adoptively transferred CD4$^+$ T cells or infected control IFN-γ$^{-/-}$ mice that did not receive CD4$^+$ T cells relative to levels in brains from naive mice. Results for each gene were calculated using the formula $2^{\wedge(\text{Average normalised naive – normalised sample})}$.

Adoptive Transfers

Splenic single cell suspensions were prepared from naive WT or RAG-1$^{-/-}$ mice, as described above. In separate experiments 40×10^6 WT splenocytes or 5×10^6 RAG-1$^{-/-}$ splenocytes (providing equivalent numbers of NK cells), were adoptively transferred into recipient mice by intravenous injection on the day before (-1) or on day 5 of *P. berghei* ANKA infection. Splenic CD4$^+$ and CD8$^+$ T lymphocytes were positively selected using anti-mouse conjugated midiMACS beads according to the manufacturer's instructions (Miltenyi Biotec). 5-10 $\times 10^6$ purified T cell populations were adoptively transferred, depending on the experiment, into recipient mice by intravenous injection on the day before (-1) or on day 5 of *P. berghei* ANKA infection. The purity and phenotype of positively selected T cell populations was assessed by flow cytometry prior to adoptive transfer and was typically found to be greater than 90%. CD4$^+$ and CD8$^+$ T cells were approximately 95% TCR αβ$^+$ and CD3$^+$. Representative plots showing the purity and heterogeneous activation status of donor CD4$^+$ T cells based upon CD44, CD62L, CD71, CD27, CXCR3 and CCR5 expression were provided for review.

Statistical analysis

The normality of all data was tested using the D'Agostino & Pearson omnibus normality test. For comparisons between 2 groups, statistical significance was determined using either a T-test or Mann Whitney Test, depending on normality of the data. For comparisons between 3 or more groups, statistical significance was determined using a one-way ANOVA with Tukey's post hoc analysis for normally distributed data or a Kruskall Wallis test with Dunn's post-hoc analysis for non-parametric data. All statistical analysis was performed using Graphpad Prism. In all cases results were classified as significantly different when P <0.05.

Results

IL-17 does not contribute to ECM during *P. berghei* ANKA infection

To assess the role of IL-17 and IFN-γ in the development of ECM we infected IFN-γ$^{-/-}$ mice, IL-17R$^{-/-}$ mice and WT control mice with *P. berghei* ANKA and monitored various parameters of infection (Figure 1). In accordance with previous observations (14, 31), all WT mice developed ECM and succumbed to infection by day 9 post-infection (p.i.), with a parasitaemia of <35% (Figure 1A, B). ECM was defined as a clinical score of 4 or 5 in the grading system described in the material and methods. In addition, WT mice showed substantial weight loss from day 7 p.i. (Figure 1C). Importantly, the course of *P. berghei* ANKA infection in IL-17R$^{-/-}$ mice, which are deficient in IL-17A and IL-17F responses, was indistinguishable from that observed in WT mice, with similar parasite burdens (except on day 9 p.i. where a higher parasitaemia was observed in IL-17R$^{-/-}$ mice) and weight loss throughout the course of infection (Figure 1A-C). All IL-17R$^{-/-}$ mice succumbed to infection by day 9 p.i. and on histological examination similar numbers of comparably sized haemorrhages were observed in the brains of IL-17R$^{-/-}$ and WT mice (Figure 1D). Furthermore, leukocyte and iRBC accumulation was observed in cerebral blood vessels of both WT and IL-17R$^{-/-}$ mice (Figure 1D). In contrast, IFN-γ$^{-/-}$ mice were protected from the development of ECM and survived to day 27 p.i. before succumbing to hyperparasitaemia and severe anaemia (Figure 1A, C and results not shown). Consistent with previous findings (7), minimal inflammation was observed in brains of IFN-γ$^{-/-}$ mice, which were removed at the time that WT and IL-17R$^{-/-}$ mice developed ECM (Figure 1D). Thus, these data confirm the essential role of IFN-γ and rule out a major role for IL-17 in the development of cerebral pathology during *P. berghei* ANKA infection.

IFN-γ is produced by multiple leukocyte populations during *P. berghei* ANKA infection

IFN-γ is crucial for the development of ECM during *P. berghei* ANKA infection (6, 7, 32), but the cellular sources of IFN-γ are unclear. Thus, to investigate whether IFN-γ is produced by multiple cell types in a temporal or organ-specific manner, or if one cell type dominates the response, we examined the kinetics of IFN-γ mRNA transcription in IFN-γ reporter (YETI) mice on various days of infection. YETI mice developed ECM and succumbed to infection with comparable kinetics as WT mice (Supplementary Figure 1). Use of reporter mice overcame problems associated with low cell recovery from the brain during infection and the need for artificial mitogenic restimulation of cells *ex vivo* to measure cytokine production. Positive and negative eYFP gates were defined using non-eYFP WT mice (results not shown). Prior to infection, approximately 10-15% of splenic T cells, 20% of lung T cells and 50% of brain-derived T cells expressed eYFP (Figure 2A, B, results not shown); these cells were all CD44$^+$ high (results not shown) and are presumably polyclonal effector/memory T cells generated under homeostatic conditions (30). The higher frequency of eYFP expression in the brain compared to spleen or lung is consistent with the notion that only effector/memory T cells perform immune surveillance within the CNS (33, 34).

There were no consistent changes in the frequencies of eYFP$^+$ CD4$^+$ and CD8$^+$ T cells in the spleen or brain until day 7 of infection, at which point the frequencies of eYFP$^+$ CD4$^+$ and CD8$^+$ T cells increased in both organs (Figure 2). Similarly the mean fluorescence intensity (MFI) of eYFP expression (measuring the number of IFN-γ transcripts and consequently their capacity to produce IFN-γ: 35) by CD4$^+$ and CD8$^+$ T cells was highest on day 7 within both organs (Figure 2D, G). Interestingly, in the brain, eYFP expression (MFI) was significantly higher by CD4$^+$ T cells compared with CD8$^+$ T cells on day 7 of infection, indicating that CD4$^+$ T cells were a greater source of IFN-γ on a cell-per-cell basis (Figure 2G). Although the frequencies of splenic CD4$^+$eYFP$^+$ and CD8$^+$eYFP$^+$ T cells were similar throughout the course of infection, significantly higher absolute numbers of CD4$^+$eYFP$^+$ T cells compared with CD8$^+$eYFP$^+$ T cells were observed in the spleen at all time-points (Figure 2E). In contrast, higher numbers of CD8$^+$eYFP$^+$ T cells were observed in the brain on day 7 of infection (Figure 2H). Numbers of eYFP$^+$ CD4$^+$ and eYFP$^+$ CD8+ T cells were similar in all organs during the earlier stages of infection (Figure 2E, H).

A high proportion (50-80%) of NK (CD3$^-$DX5$^+$) and NK-T cells (CD3$^+$DX5$^+$) constitutively expressed eYFP in the spleen and brain of naïve mice (Figure 2A, B, C, F). Neither the frequencies of eYFP$^+$NK cells nor the MFI of expression by NK cells changed significantly during the course of infection in any of the tissues, with the exception of a transient increase in MFI in the spleen on day 5 pi (Figure 2D, G and results not shown). The frequencies of eYFP$^+$NK-T cells increased slightly on 7 of infection in the spleen, but not the brain (Figure 2C, F), and the MFI of eYFP expression by NK-T cells increased on days 5 and 7 in the spleen on day 7 in the brain (Figure 2D, G and results not shown). These results are consistent with previous reports showing that resting NK and NK-T cells contain pre-formed IFN-γ mRNA and are poised for IFN-γ production (30). Nevertheless, the absolute numbers of splenic NK cells expressing eYFP did not change significantly in the brain, and declined significantly in the spleen, during infection (Figure 2E, H). The absolute numbers of NK-T cells expressing eYFP were low in comparison to the other populations and did not change significantly in any of the organs examined (Figure 2E, H).

We next analysed the total IFN-γ (eYFP) response within the spleen and brain during *P. berghei* ANKA infection to define the relative contribution of IFN-γ production from each cell type to the overall IFN-γ response (Figure 3). CD4$^+$ T cells were found to be the dominant eYFP$^+$ population in the spleen throughout the course of infection, comprising approx 50% of all eYFP$^+$ cells. The NK cell contribution to the splenic eYFP response

dropped significantly (from ~25% to < 5%) during infection, being replaced principally by CD8$^+$ T cells. NK-T cells and other cells represented ~12% of the total splenic eYFP$^+$ population throughout the course of infection (Figure 3B). NK cells were the dominant population of eYFP$^+$ cells in the brain in naive mice but were rapidly outcompeted by CD4$^+$ and CD8$^+$ T cells during infection; CD8$^+$ T cells became the dominant eYFP$^+$ population in the brain (Figure 3B). NK-T cells and other cells represented approximately 15% of the eYFP$^+$ population in the brain (Figure 3B). Combined these data show multiple cellular populations contribute to the IFN-γ response during infection and the relative contribution of each population varies with stage of infection and tissue location.

IFN-γ competent αβ$^+$CD4$^+$ T cells promote ECM in IFN-γ$^{-/-}$ recipient mice infected with *P. berghei* ANKA

Since several different cell populations can produce IFN-γ during *P. berghei* ANKA infection, we established an adoptive transfer model to examine which population(s) were the essential source(s) of IFN-γ leading to development of ECM. To demonstrate that it is possible to promote signs of ECM in IFN-γ$^{-/-}$ mice, we first adoptively transferred naïve whole splenocytes from WT mice into IFN-γ$^{-/-}$ mice one day prior to infection. 100% of IFN-γ$^{-/-}$ recipients of naive WT whole splenocytes developed prodromal signs of ECM (mean grade 2.5**:** Table 1), although none of the mice ultimately developed terminal cerebral complications. In contrast, adoptive transfer of naive splenocytes from RAG-1$^{-/-}$ mice into IFN-γ$^{-/-}$ mice failed to induce any signs of ECM (grade 1). As these results suggested the importance of T cell sources of IFN-γ in promotion of pathology, we next transferred αβ TCR$^+$ T cells purified from naive WT mice into IFN-γ$^{-/-}$ mice one day prior to infection with *P. berghei* ANKA. Importantly, adoptive transfer of naive WT TCR$^+$ T cells also promoted prodromal signs of ECM in 100% of IFN-γ$^{-/-}$ recipients (over 3 separate experiments) but the majority of animals did not progress to terminal ECM (mean grade 3.1) (Table 1). Interestingly, CD4$^+$ T cells appeared to be the most important source of pathogenic IFN-γ, as adoptive transfer of naive CD4$^+$ T cells into IFN-γ$^{-/-}$ recipients 1 day before infection conferred partial susceptibility to infection, with animals showing some prodromal signs of ECM (mean grade 2.8) (Table 1), whereas adoptive transfer of naive CD8$^+$ T cells into IFN-γ$^{-/-}$ recipients 1 day before infection did not induce any signs of ECM (grade 1). Taken together, the above data strongly indicated that CD4$^+$ T cells, and not CD8$^+$ T cells or innate cells, may be the most important source of pathogenic IFN-γ during *P. berghei* ANKA infection. However, due to the failure to induce terminal ECM in IFN-γ$^{-/-}$ mice following adoptive transfer of any population(s) of naive WT cells, we modified the model by adoptively transferring infection-derived WT leukocytes into IFN-γ$^{-/-}$ recipients. Based upon previous data showing that adoptive transfer of infection-derived WT CD8$^+$ T cells into naive CXCR3$^{-/-}$ mice immediately prior to infection promoted development of fatal cerebral malaria (11, 12), we hypothesised that this approach may provide greater sensitivity to interrogate the ability of specific IFN-γ producing cell populations to induce terminal ECM. As our initial results (above) suggested the importance of IFN-γ production by αβ TCR$^+$ T cells, we initially transferred WT αβ TCR$^+$ T cells (1:1 ratio of CD4$^+$ to CD8$^+$ T cells), harvested from spleens of infected donor mice on day 5 of *P. berghei* ANKA infection (which represents the peak of T cell expansion and activation; 31), into IFN-γ$^{-/-}$ recipients on day −1 of infection. All recipient IFN-γ$^{-/-}$ mice developed prodromal signs of ECM (mean clinical grade 3.25) but only 25% of mice that received cells on day −1 subsequently developed terminal ECM (Table 1). As expected, adoptive transfer of infection-derived (day +5) RAG-1$^{-/-}$ splenocytes into IFN-γ$^{-/-}$ recipients on day −1 of infection did not promote any signs of disease (clinical grade 1). Notably, adoptive transfer of infection-derived (day +5) αβ TCR$^+$ T cells on day +5 of infection also promoted signs of disease in 100% of recipient mice (mean clinical grade 3.75) and 50% of mice that received cells subsequently developed terminal ECM (Table 1). Combined, these data indicated that

IFN-γ production specifically by αβ TCR$^+$ T cells during the latter stages of infection (i.e. after Day 5) can cause cerebral pathology, although our data do not rule out additional roles earlier in infection. In agreement with this dual role hypothesis, adoptive transfer of infection-derived WT αβ TCR$^+$ T cells into IFN-γ $^{-/-}$ mice on day −1 and on day +5 of *P. berghei* ANKA infection induced late-stage ECM in all recipients (clinical grade 4), requiring all animals to be euthanized on day 6 or day 7 (depending on the experiment) (Table 1).

Using the same infection-derived adoptive transfer system, we next examined whether IFN-γ sufficient effector CD4$^+$ or CD8$^+$ T cell populations were individually able to promote ECM. Adoptive transfer of infection-derived (day +5) WT CD4$^+$ or CD8$^+$ T cell populations on day −1 and day +5 did not affect peripheral parasitaemia during the early stages of infection (Figure 4A). Importantly, all IFN-γ$^{-/-}$ recipients of infection-derived WT CD4$^+$ T cells developed terminal ECM and were euthanized on day 6-7 post infection (mean grade 4.6), showing similar physical signs and brain pathology as infected WT mice, including cortical and cerebellar oedema and haemorrhage (Figure 4B-D, Table 1 and Table 2). Adoptive transfer of infection-derived (day +5) CD4$^+$ T cells into IFN-γ$^{-/-}$ mice on day 5 of infection also caused prodromal signs of ECM (mean score 3.0) (Table 1). In contrast, and somewhat surprisingly, adoptive transfer of similar numbers of infection-derived WT CD8$^+$ T cells on day −1 and day +5 did not induce cerebral pathology in IFN-γ$^{-/-}$ mice and all recipients survived the acute phase of *P. berghei* ANKA infection (Figure 4B and Table 1). These experiments are the first to demonstrate that IFN-γ production solely by CD4$^+$ T cells, and not CD8$^+$ T cells or innate cells, can lead to the development of terminal ECM.

Adoptively transferred CD4$^+$ T cells migrate to lung and brain and promote ECM through active IFN-γ production

To define the mechanistic basis for the induction of ECM by WT CD4$^+$ T cells we first determined the organ/tissue localisation of adoptively transferred infection-derived CD4$^+$ T cells in recipient IFN-γ$^{-/-}$ mice. Donor Ly5.1$^+$ C57BL/6 CD4$^+$ T cells were clearly observed in the spleen, lung and brain of recipient (Ly5.2$^+$) IFN-γ$^{-/-}$ mice on day 6 or 7 of infection (depending on experiment), when the recipient mice developed ECM (Figure 5A, B). These adoptively transferred Ly5.1$^+$ CD4$^+$ T cells maintained their ability to produce IFN-γ when re-stimulated in vitro (Figure 5C, D). Importantly, neutralisation of IFN-γ production in vivo by administration of anti-IFN-γ antibody (from day −2 to day +6 of infection) completely blocked the ability of adoptively transferred CD4$^+$ T cells to induce ECM in IFN-γ$^{-/-}$ recipients (Figure 5E). These data indicate that infection-derived WT CD4$^+$ T cells promote ECM in IFN-γ$^{-/-}$ mice by secretion of IFN-γ, rather than through IFN-γ-independent effector functions imprinted during priming in an IFN-γ sufficient (WT) environment.

Adoptive transfer of infection-derived CD4$^+$ T cells does not alter the host splenic T cell response

To determine whether adoptive transfer of infection-derived IFN-γ–competent CD4$^+$ T cells modified the host's endogenous splenic T cell response, which may have contributed to the development of ECM, we assessed the ability of endogenous splenic CD4$^+$ and CD8$^+$ T cells of IFN-γ$^{-/-}$ infected mice to produce TNF (Figure 6). Although the role of TNF in promoting ECM in C57BL/6 mice during *P. berghei* ANKA infection has been questioned (36, 37), it is an informative measure of effector T cell pro-inflammatory functionality. Adoptive transfer of infection-derived WT (CD45.1$^+$) CD4$^+$ T cells did not significantly affect TNF production by host (CD45.1$^−$) splenic CD4$^+$ or CD8$^+$ T cells (Figure 6A-C); indeed host splenic CD4$^+$ T cells displayed an equivalent capacity to produce TNF during

infection compared with adoptively transferred IFN-γ-competent CD45.1$^+$ CD4$^+$ T cells (Figure 6D).

In addition, numbers of endogenous splenic CD4$^+$ and CD8$^+$ T cells were similar in IFN-$\gamma^{-/-}$ mice that either did (transfer) or did not (no transfer) receive WT CD4$^+$ T cells (Figure 6E, F) and, consistent with the lack of effect on TNF production, there were no significant differences in the frequencies of splenic CD4$^+$ or CD8$^+$ T cells that displayed an activated phenotype (CD44$^+$, CD62L^{low}, CD69$^+$, CD71$^+$ or GrB$^+$) (Figure 6G-P). Together, these data demonstrate that IFN-γ-producing CD4$^+$ T cells cause ECM directly rather than by modulating the endogenous splenic T cell response. Although we have previously shown that IFN-γ induces contraction of the splenic T cell response during *P. berghei* ANKA infection by promoting T cell apoptosis (31), adoptive transfer of IFN-γ producing CD4$^+$ T cells did not reduce endogenous splenic T cell numbers (Figure 6E, F), suggesting that the timing, concentration, location or source of IFN-γ that drives development of ECM may differ from the IFN-γ response that drives splenic T cell apoptosis.

IFN-γ–producing CD4$^+$ T cells promote ECM via CD8$^+$ T cell dependent mechanisms

Since it is well established that CD8$^+$ T cell migration to, and accumulation within, the brain is required for development of ECM in susceptible strains of mice (1, 3, 14), we hypothesised that transfer of infection-derived WT CD4$^+$ T cells would enhance accumulation of host CD8$^+$ T cells in the brains of recipient IFN-$\gamma^{-/-}$ mice. As expected, significantly higher numbers of host CD8$^+$ T cells (but not host CD4$^+$ T cells) were observed in brains of IFN-$\gamma^{-/-}$ mice that received infection-derived IFN-γ competent CD4$^+$ T cells than in brains of infected IFN-$\gamma^{-/-}$ mice that did not receive WT T cells (Figure 7A, B). In addition, although adoptive transfer of WT CD4$^+$ T cells did not affect the frequencies of brain-accumulating host CD8$^+$ T cells that expressed CD44, adoptive transfer of WT CD4$^+$ T cells did significantly increase the frequencies of brain-accumulating host CD8$^+$ T cells that were CD62L^{low}, GranzymeB$^+$ and KLRG-1$^+$, indicating that local CD4$^+$ T cell-derived IFN-γ may influence terminal differentiation and function of CD8$^+$ T cells in the brain (Figure 7C-F). As expected, antibody-induced depletion of host CD8$^+$ T cells in IFN-$\gamma^{-/-}$ mice that had received WT effector CD4$^+$ T cells, prevented the development of ECM (Figure 7G-I): anti-CD8-treated mice remained healthy until the termination of the experiment on day 14. Together, these data show that IFN-γ-producing CD4$^+$ T cells induce ECM in a CD8$^+$ T-cell dependent manner but – crucially – the CD8$^+$ T cells themselves do not need to be able to make IFN-γ.

IFN-γ competent CD4$^+$ T cells enhance the expression of pro-inflammatory chemokines in the brains of infected IFN-$\gamma^{-/-}$ mice

To determine the mechanism by which IFN-γ-competent infection-derived CD4$^+$ T cells mediate CD8$^+$ T cell accumulation within the brains of IFN-$\gamma^{-/-}$ mice during *P. berghei* ANKA infection, we compared expression of CXCL9, CXCL10, ICAM-1 and VCAM-1 mRNA in the brains of IFN-$\gamma^{-/-}$ mice that received infection-derived IFN-γ competent CD4$^+$ T cells relative to mRNA levels in control IFN-$\gamma^{-/-}$ mice that did not receive WT CD4$^+$ T cells. At the time (day 6 or day 7, depending on the experiment) when IFN-$\gamma^{-/-}$ mice that received WT CD4$^+$ T cells developed ECM, significantly higher levels of CXCL9 and CXCL10 mRNA were detected in their brains than in brains of control IFN-$\gamma^{-/-}$ mice (Figure 7J). In contrast, ICAM-1 and VCAM-1 expression was similar in the two groups of mice (Figure 7J). Importantly, neutralisation of IFN-γ significantly reduced the expression of CXCL9 and CXCL10 in the brain of IFN-$\gamma^{-/-}$ mice that received infection-derived IFN-γ competent CD4$^+$ T cells (Figure 7J). These results suggest, for the first time, that IFN-γ produced exclusively by CD4$^+$ T cells is sufficient to modulate the cerebral environment

leading to the upregulated expression of key chemokines that control pathogenic CD8^{+} T cell accumulation in the brain (10-13).

IFN-γ competent CD4^{+} T cells do not significantly increase brain parasite biomass

Adoptive transfer of infection-derived WT CD4^{+} T cells did not significantly alter the level of peripheral parasitaemia in recipient IFN-γ$^{-/-}$ mice (Figure 4A), suggesting that CD4^{+} T cells promoted ECM without significantly altering parasite burdens. Importantly, however, peripheral parasitaemia does not necessarily reflect total tissue parasite biomass (38). Thus, we specifically examined whether adoptive transfer of IFN-γ competent CD4^{+} T cells enhanced parasite sequestration/accumulation within the brain of IFN-γ$^{-/-}$ mice. Surprisingly, parasite gene expression (detecting *P. berghei* 18S and Carbamoyl phosphate synthetase genes) were not significantly increased in the brains of IFN-γ$^{-/-}$ mice that received IFN-γ competent CD4^{+} T cells compared with the levels in the brains of IFN-γ$^{-/-}$ control infected mice (Figure 8A-B). Moreover, we did not detect differences in total parasite biomass following adoptive transfer of infection-derived CD4^{+} T cells using the well established bioluminescence system (results not shown). Our results therefore suggest that IFN-γ producing CD4^{+} T cells can induce ECM development without significantly altering the overall accumulation of parasites within the brain.

Discussion

ECM has historically been considered to be an IFN-γ-dependent immunopathological syndrome. However, the discovery of Th17 cells has led to the reclassification of many conditions previously deemed to be Th1-dependent, including EAE and inflammatory arthritis (24, 25, 39). In this study, using IL-17R$^{-/-}$ mice that lack IL-17A and IL-17F responses (40), we found no evidence for a role for IL-17A or IL-17F in the development of cerebral pathology during *P. berghei* ANKA infection, which is consistent with a recent report demonstrating that IL-17(A)KO mice are susceptible to ECM development (41). These results reaffirm the pivotal and IL-17-independent role of IFN-γ in the genesis of this condition. Indeed, we did not detect Th17 responses in WT or IFN-γ$^{-/-}$ mice at any point during infection (results not shown) indicating that - even in the absence of IFN-γ, which has been reported to block Th17 cell development (42) - *P. berghei* ANKA infection fails to generate an environment suitable for Th17 differentiation.

It is perhaps unsurprising that IFN-γ mRNA (as shown by eYFP) is expressed and/or upregulated by multiple cell populations during *P. berghei* ANKA infection. Nevertheless, our study demonstrates that the cell-specific contribution to the total eYFP response is governed by both the precise stage of infection and organ of location; some cell populations upregulate eYFP within tissues whereas other eYFP[+] populations are lost. This data has important implications for not only understanding the protective and pathogenic function(s) of IFN-γ during infection but for also defining the tissue-specific signals required for the development and/or maintenance of IFN-γ producing cell populations. Although upregulation of eYFP does not guarantee that a cell will go onto to secrete IFN-γ (eYFP is a faithful marker of transcription but not translation), as *P. berghei* ANKA is an acute infection, covering only the early phases of T cell activation, it is highly probable that induction of eYFP in effector T cells reflects active protein translation (35). However, if NK cells and NK-T cells are unable to rapidly translate constitutively expressed IFN-γ mRNA during infection (30) it is possible that their contribution to the overall IFN-γ response during infection may be overestimated in our analysis.

More importantly than dissecting the sources of IFN-γ during *P. berghei* ANKA infection, we have demonstrated that IFN-γ produced solely by CD4^{+} T cells is sufficient to promote the development of ECM. Whilst we acknowledge that we were only able to induce terminal

ECM in IFN-$\gamma^{-/-}$ mice by adoptive transfer of infection-derived CD4$^+$ T cells, and not by adoptive transfer of naive CD4$^+$ T cells, we have shown that infection-derived RAG-1$^{-/-}$ cells and infection-derived WT CD8$^+$ T cells are unable to promote any signs of ECM when adoptively transferred into IFN-$\gamma^{-/-}$ mice. Moreover, we have shown that naive WT CD4$^+$ T cells, but not naive RAG-1$^{-/-}$ cells nor naive WT CD8$^+$ T cells, promote comparable levels of disease as whole naive splenocytes when adoptively transferred into IFN-$\gamma^{-/-}$ mice. Thus, when our naive and infection-derived adoptive transfer results are combined, our data very convincingly show that CD4$^+$ T cells are the predominant source of pathogenic IFN-γ during *P. berghei* ANKA infection. Whilst previous studies have shown that CD4$^+$ T cells are involved in the development of ECM (7, 43-45), this is the first definitive proof that they do so specifically through IFN-γ production. The inability of naive cell transfers to induce ECM is potentially related to the specific immunological conditions induced during *P. berghei* ANKA infection, which possibly prevents the priming, maintenance and survival of sufficient numbers of transferred cells in the recipient mice to cause ECM. Indeed, we and others have previously described the pro-apoptotic environment induced by *P. berghei* ANKA infection (31, 46), which causes the contraction of the T cell effector response.

CD4$^+$ T cells, rather than CD8$^+$ T cells, may be the most important source of IFN-γ during *P. berghei* ANKA infection simply because – in the brain, at least - they produce much more IFN-γ on a per-cell basis than do CD8$^+$ T cells. But it is also possible that CD4$^+$ and CD8$^+$ T cells accumulate in different anatomical locations within the brain, for example in the subarachnoid space or perivascular spaces, where localised IFN-γ production is more – or less - damaging. Crucially, however, we have shown that IFN-γ-producing CD4$^+$ T cells cannot, by themselves, induce ECM in IFN-$\gamma^{-/-}$ mice; adoptive transfer of IFN-γ-producing CD4$^+$ T cells into infected IFN-$\gamma^{-/-}$ mice increased endogenous CD8$^+$ T cell accumulation within the brain and depletion of endogenous CD8$^+$ T cells prevented onset of ECM. Thus, our data indicate that IFN-γ-producing CD4$^+$ T cells drive the development of ECM during *P. berghei* ANKA infection by facilitating the entry and accumulation of CD8$^+$ T cells into the brain, which then mediate pathology through IFN-γ independent mechanisms.

Although it has recently been shown that CD4$^+$ T cells are required for the activation of pathogenic CD8$^+$ T cells during *P. berghei* ANKA infection (45), we do not believe that IFN-γ producing CD4$^+$ T cells simply activate CD8$^+$ T cells in the lymphoid compartment or periphery during infection, allowing their migration to the CNS, since transfer of WT infection-derived CD8$^+$ T cells (which were primed in the presence of IFN-γ sufficient CD4$^+$ T cells) was not sufficient to induce ECM. Although it is possible that IFN-γ producing CD4$^+$ T cells directly modulate CD8$^+$ T cell effector function after day 5 of infection - when the CD8$^+$ T cells were purified for adoptive transfer - we do not believe this to be likely as the activation and effector functions of splenic, brain and lung infiltrating CD8$^+$ T cells are seemingly unimpaired in IFN-$\gamma^{-/-}$ mice on day 7 of infection, when WT mice develop ECM (31). These data, when taken together with our finding here that adoptive transfer of WT CD4$^+$ T cells into infected IFN-$\gamma^{-/-}$ mice leads to upregulation of the chemokines CXCL9 and CXCL10 within the brain, leads us to conclude that the major role of IFN-γ–secreting CD4$^+$ T cells, which accumulate in the brain through IFN-γ independent mechanisms (31), is to modulate the localised brain environment, facilitating the migration/accumulation of CD8$^+$ T cells into the brain. This hypothesis is consistent with upregulation of genes associated with interferon-signalling in the brains of ECM-susceptible mice infected with *P. berghei* ANKA (8, 9) and with studies showing much lower expression of CXCL9 and CXCL10 in brains of ECM-resistant IFN-$\gamma^{-/-}$ mice than in brains of susceptible WT mice during *P. berghei* ANKA infection (7, 10, 31). The CD8$^+$ T cell effector mechanisms responsible for progression to end-stage ECM are poorly understood; the data presented here indicate that CD8$^+$ T cells do not need to produce IFN-γ

- which is in agreement with a very recent study indicating that CD8$^+$ T cells do not need to express IFN-γ for their accumulation or pathogenic function within the brain (47) - but evidence from other studies indicates a role for Granzyme B-dependent and perforin-mediated killing of brain endothelial cells (47-49).

We have also shown that adoptive transfer of IFN-γ producing CD4$^+$ T cells does not affect total parasite transcript levels within the brain of IFN-$\gamma^{-/-}$ mice during *P. berghei* ANKA infection. We also failed to detect differences in parasite biomass using the bioluminescence system, as utilised by Amante et al (16) and Claser et al (15) (results not shown but provided for review). These results are surprising as a number of recent studies have shown that IFN-γ dependent parasite accumulation in the brain is a key feature of ECM and is necessary for development of pathology (15, 16, 49-51). There is, however, some debate on the precise role of CD4$^+$ T cells in mediating parasite accumulation within tissues during *P. berghei* ANKA infection; Amante *et al* (16) have recently suggested that CD4$^+$ T cells are required for parasite accumulation within tissues whereas Claser *et al* (15) reported that CD4$^+$ T cells do not facilitate parasite accumulation within the brain. Nonetheless, our results suggest that in our ECM model extensive parasite accumulation within the brain is not essential for the development of cerebral pathology, which may underline the heterogeneity of the ECM syndrome. However, whilst adoptive transfer of CD4$^+$ T cells did not significantly increase total parasite levels within the brain, elevated accumulation within specific and small regions of the brain would not necessarily have been detected in our analysis. In this scenario, parasite accumulation within a small number of specific and focal regions may have been sufficient to cause ECM. Crucially, we do not yet understand the precise regions of the brain that are most sensitive to parasite accumulation and inflammation during malaria infection, leading to death (52). Identifying if (and how) *P. berghei* ANKA parasites sequester within the brain microvessels and the relative importance of this process for development of ECM is an ongoing area of research in our and other laboratories.

In summary, we have examined the cellular sources of IFN-γ during *P. berghei* ANKA infection and we have highlighted, for the first time, that CD4$^+$ T cells promote the development of ECM specifically through their production of IFN-γ. Our results suggest that IFN-γ produced by CD4$^+$ T cells may act locally within the brain to modify the brain environment, which is required for accumulation of CD8$^+$ T cells within the brain, leading to ECM. These data represent a significant advance in our understanding of the pathogenesis of ECM during *P. berghei* ANKA infection which may have implications for understanding – and therefore either preventing or treating – human cerebral malaria.

Supplementary Material

Refer to Web version on PubMed Central for supplementary material.

Acknowledgments

References

1. de Souza JB, Hafalla JC, Riley EM, Couper KN. Cerebral malaria: why experimental murine models are required to understand the pathogenesis of disease. Parasitology. 2010; 137:755–772. [PubMed: 20028608]

2. Riley EM, Couper KN, Helmby H, Hafalla JC, de Souza JB, Langhorne J, Jarra WB, Zavala F. Neuropathogenesis of human and murine malaria. Trends Parasitol. 2010; 26:277–278. [PubMed: 20338809]

3. Good MF, Xu H, Wykes M, Engwerda CR. Development and regulation of cell-mediated immune responses to the blood stages of malaria: implications for vaccine research. Annu Rev Immunol. 2005; 23:69–99. [PubMed: 15771566]

4. Dai M, Reznik SE, Spray DC, Weiss LM, Tanowitz HB, Gulinello M, Desruisseaux MS. Persistent cognitive and motor deficits after successful antimalarial treatment in murine cerebral malaria. Microbes Infect. 2010; 12:1198–1207. [PubMed: 20800692]

5. Reis PA, Comim CM, Hermani F, Silva B, Barichello T, Portella AC, Gomes FC, Sab IM, Frutuoso VS, Oliveira MF, Bozza PT, Bozza FA, Dal-Pizzol F, Zimmerman A, Quevedo J, Castro-Faria-Neto HC. Cognitive dysfunction is sustained after rescue therapy in experimental cerebral malaria, and is reduced by additive antioxidant therapy. PLoS Pathog. 2010; 6:e1000963. [PubMed: 20585569]

6. Amani V, Vigario AM, Belnoue E, Marussig M, Fonseca L, Mazier D, Renia L. Involvement of IFN-gamma receptor-medicated signaling in pathology and anti-malarial immunity induced by Plasmodium berghei infection. Eur J Immunol. 2000; 30:1646–1655. [PubMed: 10898501]

7. Belnoue E, Potter SM, Rosa DS, Mauduit M, Gruner AC, Kayibanda M, Mitchell AJ, Hunt NH, Renia L. Control of pathogenic CD8+ T cell migration to the brain by IFN-gamma during experimental cerebral malaria. Parasite Immunol. 2008; 30:544–553. [PubMed: 18665903]

8. Miu J, Hunt NH, Ball HJ. Predominance of interferon-related responses in the brain during murine malaria, as identified by microarray analysis. Infect Immun. 2008; 76:1812–1824. [PubMed: 18299338]

9. Lovegrove FE, Gharib SA, Patel SN, Hawkes CA, Kain KC, Liles WC. Expression microarray analysis implicates apoptosis and interferon-responsive mechanisms in susceptibility to experimental cerebral malaria. Am J Pathol. 2007; 171:1894–1903. [PubMed: 17991715]

10. Van den Steen PE, Deroost K, Van Aelst I, Geurts N, Martens E, Struyf S, Nie CQ, Hansen DS, Matthys P, Van Damme J, Opdenakker G. CXCR3 determines strain susceptibility to murine cerebral malaria by mediating T lymphocyte migration toward IFN-gamma-induced chemokines. Eur J Immunol. 2008; 38:1082–1095. [PubMed: 18383042]

11. Miu J, Mitchell AJ, Muller M, Carter SL, Manders PM, McQuillan JA, Saunders BM, Ball HJ, Lu B, Campbell IL, Hunt NH. Chemokine gene expression during fatal murine cerebral malaria and protection due to CXCR3 deficiency. J Immunol. 2008; 180:1217–1230. [PubMed: 18178862]

12. Campanella GS, Tager AM, El Khoury JK, Thomas SY, Abrazinski TA, Manice LA, Colvin RA, Luster AD. Chemokine receptor CXCR3 and its ligands CXCL9 and CXCL10 are required for the development of murine cerebral malaria. Proc Natl Acad Sci U S A. 2008; 105:4814–4819. [PubMed: 18347328]

13. Nie CQ, Bernard NJ, Norman MU, Amante FH, Lundie RJ, Crabb BS, Heath WR, Engwerda CR, Hickey MJ, Schofield L, Hansen DS. IP-10-mediated T cell homing promotes cerebral inflammation over splenic immunity to malaria infection. PLoS Pathog. 2009; 5:e1000369. [PubMed: 19343215]

14. Belnoue E, Kayibanda M, Vigario AM, Deschemin JC, van Rooijen N, Viguier M, Snounou G, Renia L. On the pathogenic role of brain-sequestered alphabeta CD8+ T cells in experimental cerebral malaria. J Immunol. 2002; 169:6369–6375. [PubMed: 12444144]

15. Claser C, Malleret B, Gun SY, Wong AY, Chang ZW, Teo P, See PC, Howland SW, Ginhoux F, Renia L. CD8+ T cells and IFN-gamma mediate the time-dependent accumulation of infected red blood cells in deep organs during experimental cerebral malaria. PLoS One. 2011; 6:e18720. [PubMed: 21494565]

16. Amante FH, Haque A, Stanley AC, Rivera Fde L, Randall LM, Wilson YA, Yeo G, Pieper C, Crabb BS, de Koning-Ward TF, Lundie RJ, Good MF, Pinzon-Charry A, Pearson MS, Duke MG, McManus DP, Loukas A, Hill GR, Engwerda CR. Immune-mediated mechanisms of parasite tissue sequestration during experimental cerebral malaria. J Immunol. 2010; 185:3632–3642. [PubMed: 20720206]

17. McCall MB, Sauerwein RW. Interferon-gamma--central mediator of protective immune responses against the pre-erythrocytic and blood stage of malaria. J Leukoc Biol. 2010; 88:1131–1143. [PubMed: 20610802]

18. Schroder K, Hertzog PJ, Ravasi T, Hume DA. Interferon-gamma: an overview of signals, mechanisms and functions. J Leukoc Biol. 2004; 75:163–189. [PubMed: 14525967]

19. Horowitz A, Newman KC, Evans JH, Korbel DS, Davis DM, Riley EM. Cross-talk between T cells and NK cells generates rapid effector responses to Plasmodium falciparum-infected erythrocytes. J Immunol. 2010; 184:6043–6052. [PubMed: 20427769]

20. Perry JA, Olver CS, Burnett RC, Avery AC. Cutting edge: the acquisition of TLR tolerance during malaria infection impacts T cell activation. J Immunol. 2005; 174:5921–5925. [PubMed: 15879082]

21. Sponaas AM, Cadman ET, Voisine C, Harrison V, Boonstra A, O'Garra A, Langhorne J. Malaria infection changes the ability of splenic dendritic cell populations to stimulate antigen-specific T cells. J Exp Med. 2006; 203:1427–1433. [PubMed: 16754719]

22. Mitchell AJ, Hansen AM, Hee L, Ball HJ, Potter SM, Walker JC, Hunt NH. Early cytokine production is associated with protection from murine cerebral malaria. Infect Immun. 2005; 73:5645–5653. [PubMed: 16113282]

23. O'Connor RA, Prendergast CT, Sabatos CA, Lau CW, Leech MD, Wraith DC, Anderton SM. Cutting edge: Th1 cells facilitate the entry of Th17 cells to the central nervous system during experimental autoimmune encephalomyelitis. J Immunol. 2008; 181:3750–3754. [PubMed: 18768826]

24. Veldhoen M, Hocking RJ, Flavell RA, Stockinger B. Signals mediated by transforming growth factor-beta initiate autoimmune encephalomyelitis, but chronic inflammation is needed to sustain disease. Nat Immunol. 2006; 7:1151–1156. [PubMed: 16998492]

25. Bettelli E, Carrier Y, Gao W, Korn T, Strom TB, Oukka M, Weiner HL, Kuchroo VK. Reciprocal developmental pathways for the generation of pathogenic effector TH17 and regulatory T cells. Nature. 2006; 441:235–238. [PubMed: 16648838]

26. Siffrin V, Radbruch H, Glumm R, Niesner R, Paterka M, Herz J, Leuenberger T, Lehmann SM, Luenstedt S, Rinnenthal JL, Laube G, Luche H, Lehnardt S, Fehling HJ, Griesbeck O, Zipp F. In vivo imaging of partially reversible th17 cell-induced neuronal dysfunction in the course of encephalomyelitis. Immunity. 2010; 33:424–436. [PubMed: 20870176]

27. Kebir H, Kreymborg K, Ifergan I, Dodelet-Devillers A, Cayrol R, Bernard M, Giuliani F, Arbour N, Becher B, Prat A. Human TH17 lymphocytes promote blood-brain barrier disruption and central nervous system inflammation. Nat Med. 2007; 13:1173–1175. [PubMed: 17828272]

28. Das Sarma J, Ciric B, Marek R, Sadhukhan S, Caruso ML, Shafagh J, Fitzgerald DC, Shindler KS, Rostami A. Functional interleukin-17 receptor A is expressed in central nervous system glia and upregulated in experimental autoimmune encephalomyelitis. J Neuroinflammation. 2009; 6:14. [PubMed: 19400960]

29. Ma X, Reynolds SL, Baker BJ, Li X, Benveniste EN, Qin H. IL-17 enhancement of the IL-6 signaling cascade in astrocytes. J Immunol. 2010; 184:4898–4906. [PubMed: 20351184]

30. Stetson DB, Mohrs M, Reinhardt RL, Baron JL, Wang ZE, Gapin L, Kronenberg M, Locksley RM. Constitutive cytokine mRNAs mark natural killer (NK) and NK T cells poised for rapid effector function. J Exp Med. 2003; 198:1069–1076. [PubMed: 14530376]

31. Villegas-Mendez A, de Souza JB, Murungi L, Hafalla JC, Shaw TN, Greig R, Riley EM, Couper KN. Heterogeneous and tissue-specific regulation of effector T cell responses by IFN-gamma during Plasmodium berghei ANKA infection. J Immunol. 2011; 187:2885–2897. [PubMed: 21880980]

32. Grau GE, Heremans H, Piguet PF, Pointaire P, Lambert PH, Billiau A, Vassalli P. Monoclonal antibody against interferon gamma can prevent experimental cerebral malaria and its associated overproduction of tumor necrosis factor. Proc Natl Acad Sci U S A. 1989; 86:5572–5574. [PubMed: 2501793]

33. Kwok LY, Miletic H, Lutjen S, Soltek S, Deckert M, Schluter D. Protective immunosurveillance of the central nervous system by Listeria-specific CD4 and CD8 T cells in systemic listeriosis in the absence of intracerebral Listeria. J Immunol. 2002; 169:2010–2019. [PubMed: 12165527]

34. Wilson EH, Weninger W, Hunter CA. Trafficking of immune cells in the central nervous system. J Clin Invest. 2010; 120:1368–1379. [PubMed: 20440079]

35. Mayer KD, Mohrs K, Crowe SR, Johnson LL, Rhyne P, Woodland DL, Mohrs M. The functional heterogeneity of type 1 effector T cells in response to infection is related to the potential for IFN-gamma production. J Immunol. 2005; 174:7732–7739. [PubMed: 15944275]

36. Grau GE, Fajardo LF, Piguet PF, Allet B, Lambert PH, Vassalli P. Tumor necrosis factor (cachectin) as an essential mediator in murine cerebral malaria. Science. 1987; 237:1210–1212. [PubMed: 3306918]

37. Engwerda CR, Mynott TL, Sawhney S, de Souza JB, Bickle QD, Kaye PM. Locally up-regulated lymphotoxin alpha, not systemic tumor necrosis factor alpha, is the principle mediator of murine cerebral malaria. J Exp Med. 2002; 195:1371–77. [PubMed: 12021316]

38. Franke-Fayard B, Fonager J, Braks A, Khan SM, Janse CJ. Sequestration and tissue accumulation of human malaria parasites: can we learn anything from rodent models of malaria? PLoS Pathog. 2010; 6:e1001032. [PubMed: 20941396]

39. Toy D, Kugler D, Wolfson M, Vanden Bos T, Gurgel J, Derry J, Tocker J, Peschon J. Cutting edge: interleukin 17 signals through a heteromeric receptor complex. J Immunol. 2006; 177:36–39. [PubMed: 16785495]

40. Sarkar S, Cooney LA, Fox DA. The role of T helper type 17 cells in inflammatory arthritis. Clin Exp Immunol. 2010; 159:225–237. [PubMed: 19758374]

41. Ishida H, Matsuzaki-Moriya C, Imai T, Yanagisawa K, Nojima Y, Suzue K, Hirai M, Iwakura Y, Yoshimura A, Hamano S, Shimokawa C, Hisaeda H. Development of experimental cerebral malaria is independent of IL-23 and IL-17. Biochem Biophys Res Commun. 2010; 402:790–795. [PubMed: 21036146]

42. Harrington LE, Hatton RD, Mangan PR, Turner H, Murphy TL, Murphy KM, Weaver CT. Interleukin 17-producing CD4+ effector T cells develop via a lineage distinct from the T helper type 1 and 2 lineages. Nat Immunol. 2005; 6:1123–1132. [PubMed: 16200070]

43. Grau GE, Piguet PF, Engers HD, Louis JA, Vassalli P, Lambert PH. L3T4+ T lymphocytes play a major role in the pathogenesis of murine cerebral malaria. J Immunol. 1986; 137:2348–2354. [PubMed: 3093572]

44. Yanez DM, Manning DD, Cooley AJ, Weidanz WP, van der Heyde HC. Participation of lymphocyte subpopulations in the pathogenesis of experimental murine cerebral malaria. J Immunol. 1996; 157:1620–1624. [PubMed: 8759747]

45. Haque A, Best SE, Ammerdorffer A, Desbarrieres L, de Oca MM, Amante FH, de Labastida Rivera F, Hertzog P, Boyle GM, Hill GR, Engwerda CR. Type I Interferons suppress CD4(+) T cell-dependent parasite control during blood-stage Plasmodium infection. Eur J Immunol. 2011

46. Hirunpetcharat C, Good MF. Deletion of Plasmodium berghei-specific CD4+ T cells adoptively transferred into recipient mice after challenge with homologous parasite. Proc Natl Acad Sci U S A. 1998; 17:1715–20. [PubMed: 9465082]

47. Haque A, Best SE, Unosson K, Amante FH, de Labastida F, Anstey NM, Karupiah G, Smyth MJ, Heath WR, Engwerda CR. Granzyme B expression by CD8+ T cells is required for the development of experimental cerebral malaria. J Immunol. 2011; 186:6148–6156. [PubMed: 21525386]

48. Potter S, Chan-Ling T, Ball HJ, Mansour H, Mitchell A, Maluish L, Hunt NH. Perforin mediated apoptosis of cerebral microvascular endothelial cells during experimental cerebral malaria. Int J Parasitol. 2006; 36:485–496. [PubMed: 16500656]

49. Nitcheu J, Bonduelle O, Combadiere C, Tefit M, Seilhean D, Mazier D, Combadiere B. Perforin-dependent brain-infiltrating cytotoxic CD8+ T lymphocytes mediate experimental cerebral malaria pathogenesis. J Immunol. 2003; 170:2221–2228. [PubMed: 12574396]

50. McQuillan JA, Mitchell AJ, Ho YF, Combes V, Ball HJ, Golenser J, Grau GE, Hunt NH. Coincident parasite and CD8 T cell sequestration is required for development of experimental cerebral malaria. Int J Parasitol. 2011; 41:155–163. [PubMed: 20828575]

51. Baptista FG, Pamplona A, Pena AC, Mota MM, Pied S, Vigario AM. Accumulation of Plasmodium berghei-infected red blood cells in the brain is crucial for the development of cerebral malaria in mice. Infect Immun. 2010; 78:4033–4039. [PubMed: 20605973]

52. Haldar K, Murphy SC, Milner DA, Taylor TE. Malaria: mechanisms of erythrocytic infection and pathological correlates of severe disease. Annu Rev Pathol. 2007; 2:217–249. [PubMed: 18039099]
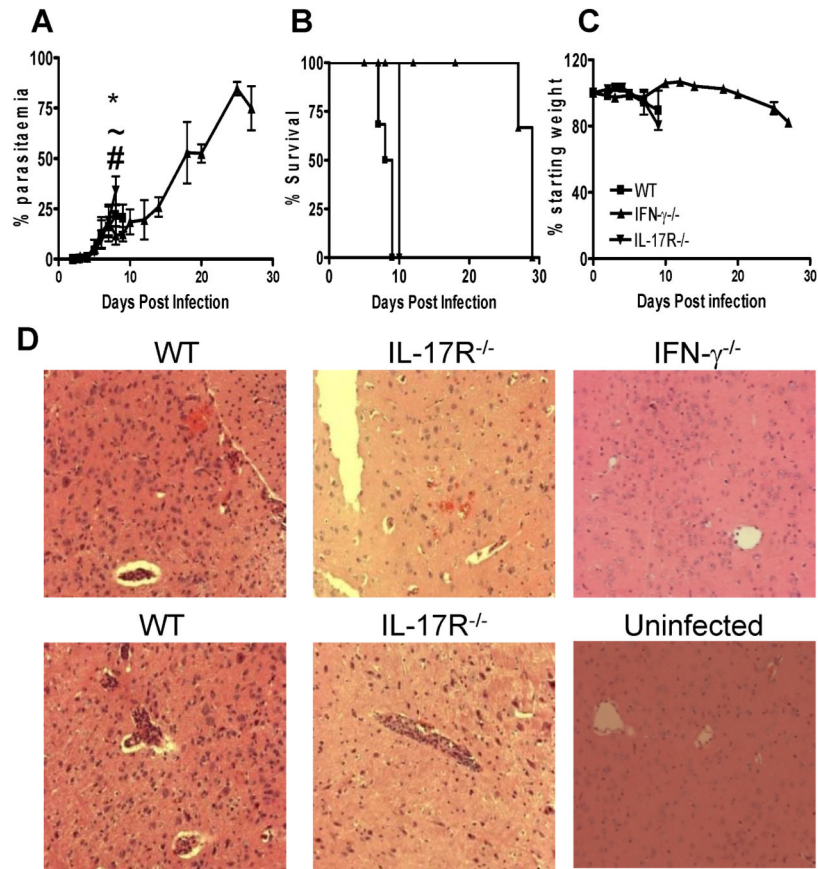
Figure 1. IFN-γ promotes ECM independently from IL-17

WT, IFN-$\gamma^{-/-}$ and IL-17R$^{-/-}$ mice were infected i.v. with 10^4 *P. berghei* ANKA pRBC. (A-C) The course of infection was assessed by monitoring (A) peripheral parasitaemia, (B) mortality and (C) weight loss. (D) Histological (H & E) staining of brain sections (cortex) demonstrating severity of cerebral pathology on day 8-9 of infection. The results are representative of two independent experiments with 3-5 mice per group. * P<0.05 between WT and IFN-$\gamma^{-/-}$ mice; ~ P<0.05 between WT and IL-17R$^{-/-}$ mice; # P<0.05 between IFN-$\gamma^{-/-}$ and IL-17R$^{-/-}$ mice.
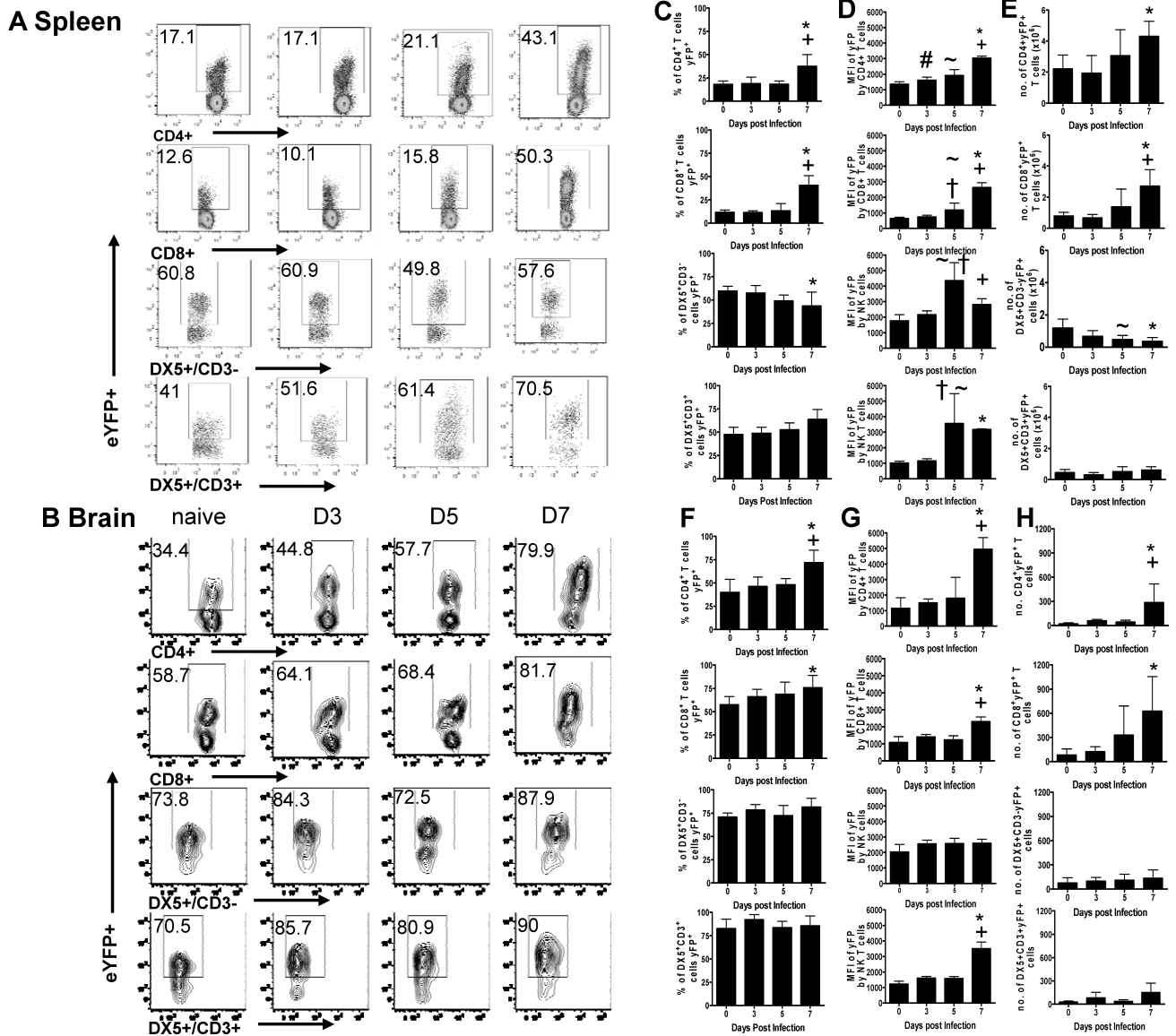
Figure 2. Multiple cell populations produce IFN-γ during *P. berghei* ANKA infection

IFN-γ eYFP reporter mice (YETI) were infected i.v. with 10^4 *P. berghei* ANKA pRBC. (A, B) Representative plots showing eYFP expression by CD4+, CD8+ T cells, NK cells (CD3−DX5+) and NK T cells (CD3+DX5+) in the spleen (A), and brain (B) of naive mice and on days 3, 5 and 7 of infection. (C-H) The frequencies (C, F), Mean fluorescence intensity (D, G) and total numbers (E, H) of IFN-γ expressing cells within the spleen (C-E) and brain (F-H). The results are the mean +/− SD of the group with 3-4 mice per group. The results are representative of 3 separate experiments. # P<0.05 between D0 and D3; ~ P<0.05 between D0 and D5; * P<0.05 between D0 and D7; † P<0.05 between D3 and D5; + P<0.05 between D5 and D7
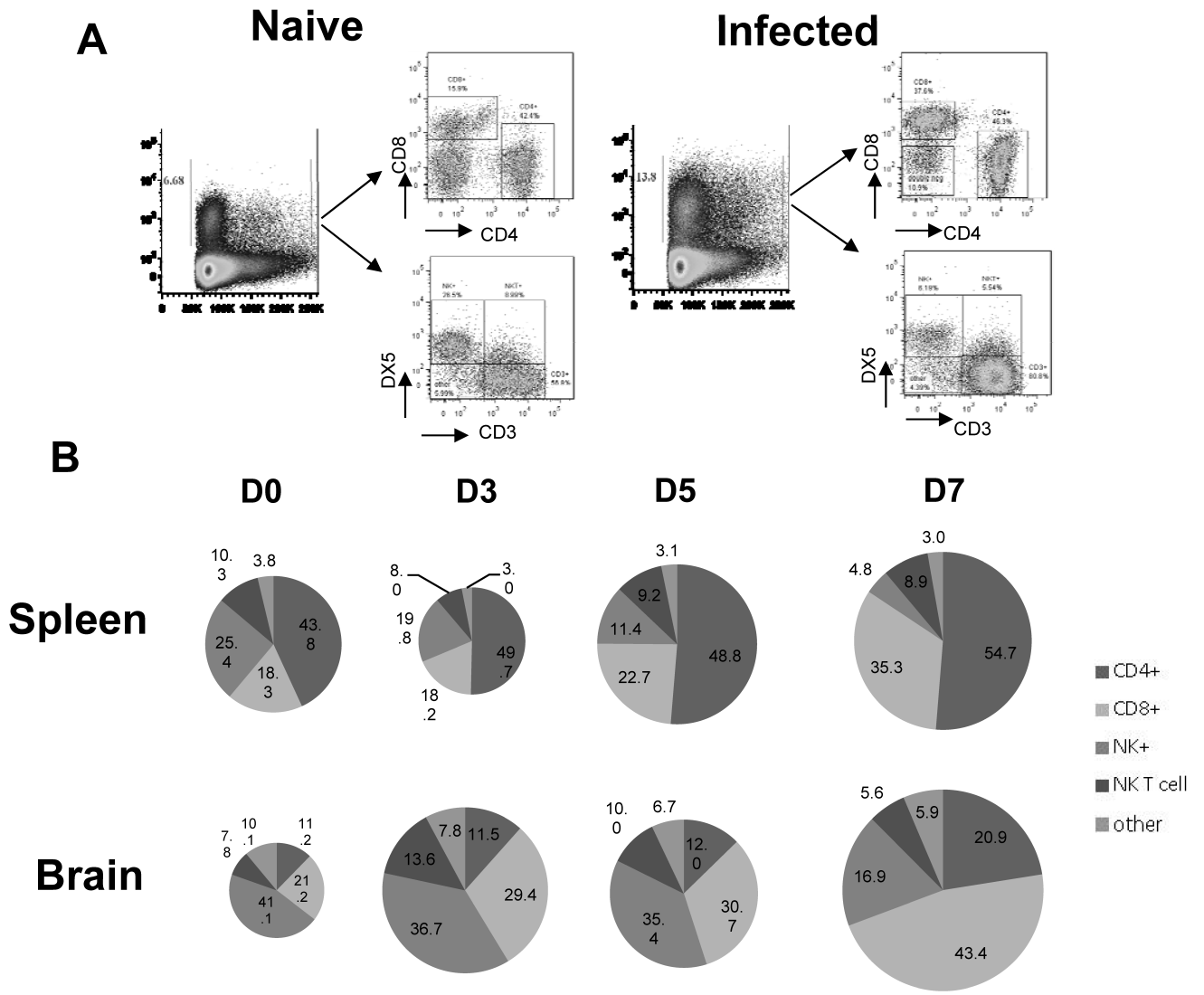
Figure 3. Temporal changes in cellular contribution to total IFN-γ response during infection
IFN-γ eYFP reporter mice (YETI) were infected i.v. with 10^4 *P. berghei* ANKA pRBC. (A)
Representative plots showing the differentiation of cellular subsets within the total splenic
eYFP response. (B) Pie charts showing the relative contribution of specific cellular
populations to the total eYFP response in the spleen and brain in naive mice and on days 3, 5
and 7 of infection. The results are the mean of the group with 3-4 mice per group. The
results are representative of 2 separate experiments.
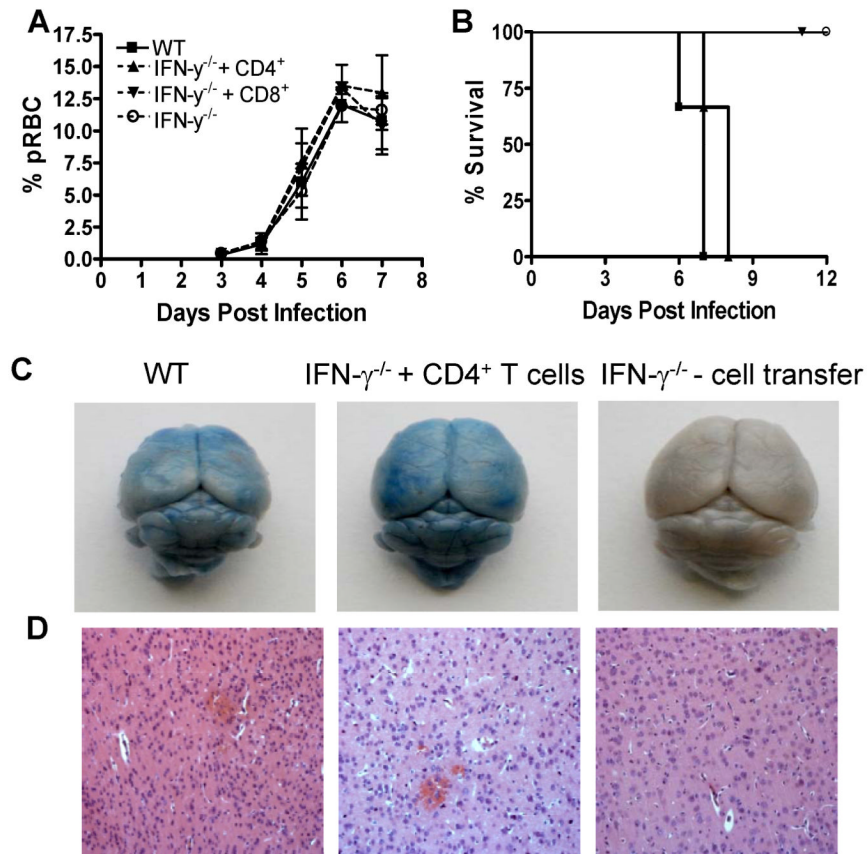
**Figure 4. Infection-derived IFN-γ competent CD4+ T cells promote ECM in IFN-γ−/− mice infected with *P. berghei* ANKA**

CD4+ and CD8+ T cells were purified from C57BL/6 mice on day 5 of *P. berghei* ANKA infection (10^4 pRBC i.v.) and were adoptively transferred (i.v.) separately into recipient IFN-γ−/− mice one day prior to infection with *P. berghei* ANKA (10^4 pRBC i.v.). A secondary adoptive transfer (i.v.) of day 5 infection-derived C57BL/6 CD4+ or CD8+ T cells into recipient IFN-γ−/− mice was performed on day 5 of infection. The course of infection was assessed by monitoring (A) peripheral parasitaemia and (B) mortality. The severity of cerebral pathology was determined on day 7 of infection by assessing (C) the extravasation of evans blue within the brain parenchyma and (D) histological (H & E) staining. The results are the mean +/− SD of the group with 3-4 mice per group. The results are representative of 5 separate experiments.
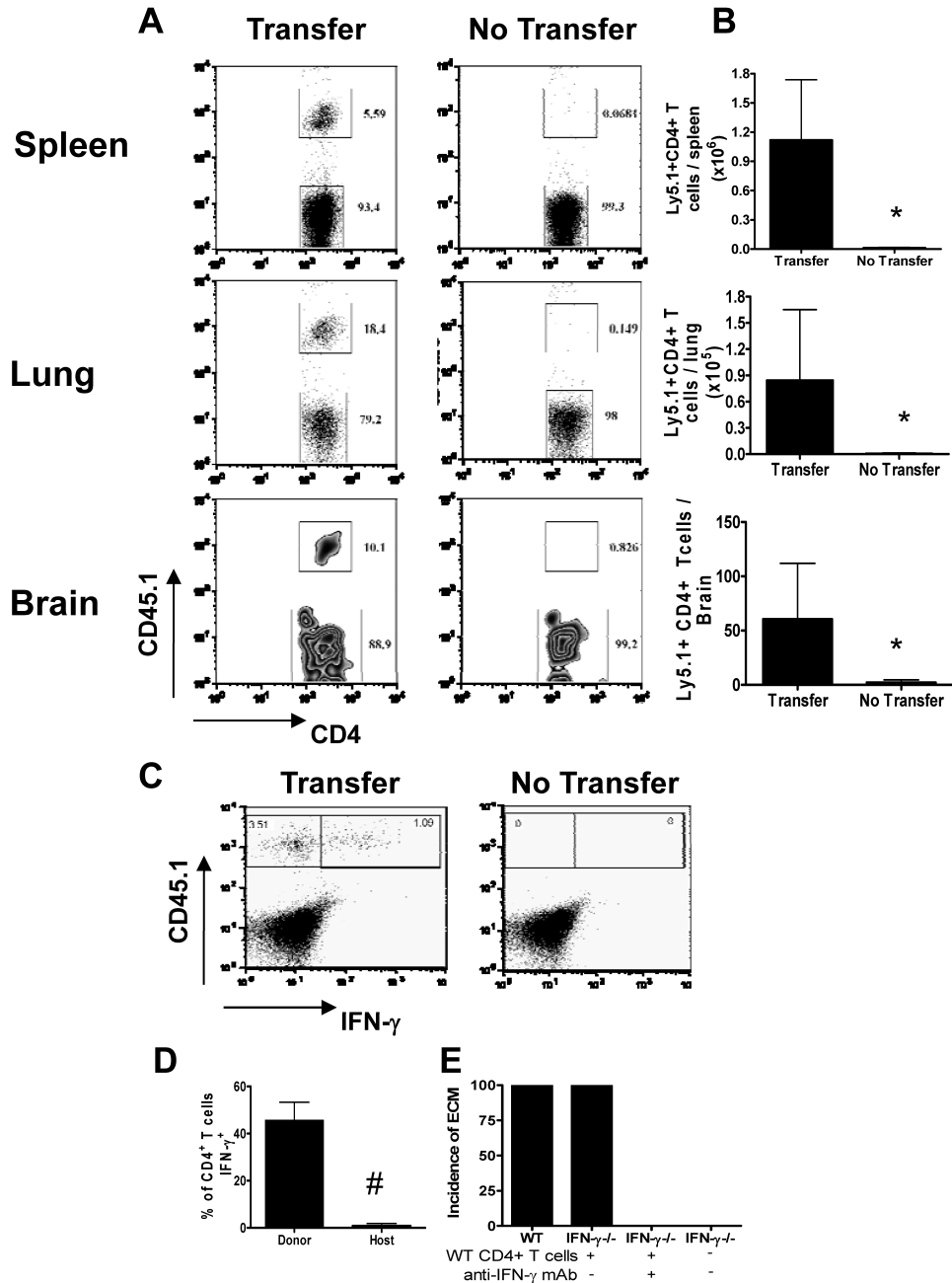
Figure 5. Adoptively transferred infection-derived IFN-γ producing CD4^{+} T cells accumulate in lymphoid and non-lymphoid tissues and induce ECM in IFN-γ^{−/−} mice through active production of IFN-γ

CD4^{+} T cells were purified from CD45.1^{+}C57BL/6 mice on day 5 of *P. berghei* ANKA infection (10^4 pRBC i.v.) and were adoptively transferred (i.v.) into recipient CD45.2[+]IFN-γ^{−/−} mice one day prior to infection with *P. berghei* ANKA (10^4 pRBC i.v.). A secondary adoptive transfer (i.v.) of day 5 infection-derived CD45.1^{+}C57BL/6 CD4^{+} T cells into recipient IFN-γ^{−/−} mice was performed on day 5 of infection. (A) Representative plots (gated on CD4^{+} T cells) showing the recovery of host (CD45.1^{−}) and donor (CD45.1^{+}) CD4^{+} T cells within the spleen, lung and brain on day 7 of infection. (B) The numbers of

recovered adoptively transferred cells within the spleen, lung and brain. (C) Representative plots showing the production of IFN-γ by donor and host CD4$^+$ T cells within the spleen on day 7 of infection. (D) The frequency of donor and host CD4$^+$ T cells producing IFN-γ on day 7 of infection within the spleen. (E) The incidence of ECM in recipient and control IFN-$\gamma^{-/-}$ mice and recipient IFN-$\gamma^{-/-}$ mice treated with anti-IFN-γ Ab on days -2, 0, 2, 4 and 6. The results are the mean $+/-$ SD of the group with 3-4 mice per group. The results are representative of 2 separate experiments. (B) * P<0.05 between infected IFN-$\gamma^{-/-}$ recipients of WT cells and infected IFN-$\gamma^{-/-}$ controls; (D) # P<0.05 between donor CD4$^+$ T cells and host CD4$^+$ T cells.
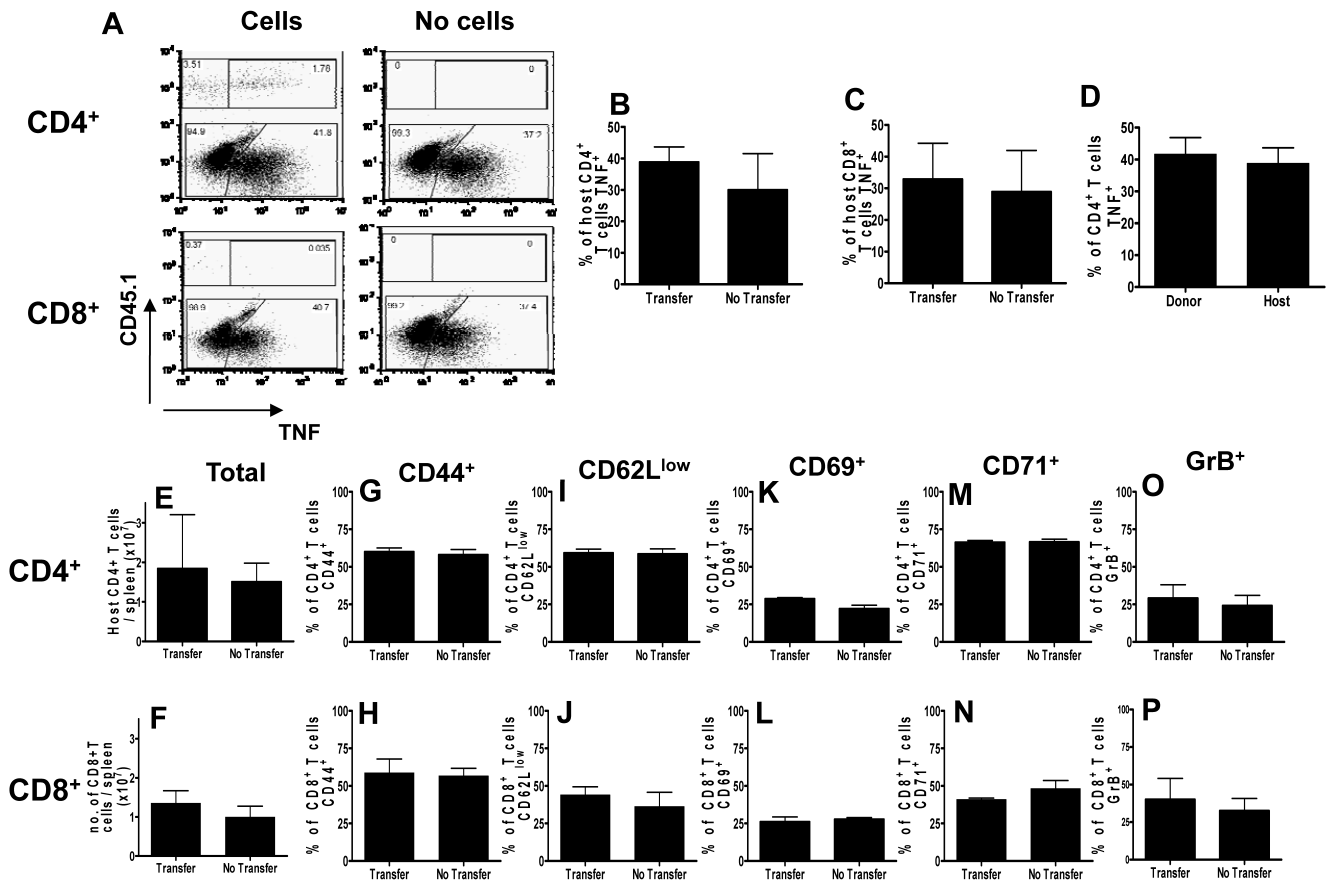
Figure 6. Adoptively transferred infection-derived IFN-γ producing CD4^{+} T cells do not alter host splenic CD4^{+} or CD8^{+} T cell responses in IFN-γ^{−/−} mice during *P. berghei* ANKA infection

CD4^{+} T cells were purified from CD45.1^{+}C57BL/6 mice on day 5 of *P. berghei* ANKA infection (10^4 pRBC i.v.) and were adoptively transferred (i.v.) into recipient CD45.2[+]IFN-γ^{−/−} mice one day prior to infection with *P. berghei* ANKA (10^4 pRBC i.v.). A secondary adoptive transfer (i.v.) of day 5 infection-derived CD45.1^{+}C57BL/6 CD4^{+} T cells into recipient IFN-γ^{−/−} mice was performed on day 5 of infection. (A) Representative plots showing the production of TNF by donor and host CD4^{+} T cells and host CD8^{+} T cells within the spleen on day 7 of infection. (B) The frequency of host splenic CD4^{+} T cells producing TNF in adoptive transfer-recipient (transfer) and control IFN-γ^{−/−} mice (no transfer) mice. (C) The frequency of host splenic CD8^{+} T cells producing TNF in adoptive transfer-recipient (transfer) and control IFN-γ^{−/−} mice (no transfer) mice. (D) The frequency of donor (CD45.1^{+}) and host (CD45.1^{−}) CD4^{+} T cells producing TNF in the spleen of recipient IFN-γ^{−/−} mice. (E-P) The number of total host splenic (E) CD4^{+} and (F) CD8^{+} T cells. (G-P) the frequencies of activated host splenic CD4^{+} (G, I, K, M, O) and CD8^{+} (H, J, L, N, P) T cells expressing CD44^{+} (G, H), CD62L^{low} (I, J), CD69^{+} (K, L) CD71^{+} (M, N) and GrB^{+} (O, P) within the spleen of adoptive transfer-recipient (transfer) and control IFN-γ^{−/−} mice (no transfer) mice. The results are the mean +/− SD of the group with 3-4 mice per group. The results are representative of 3 separate experiments.
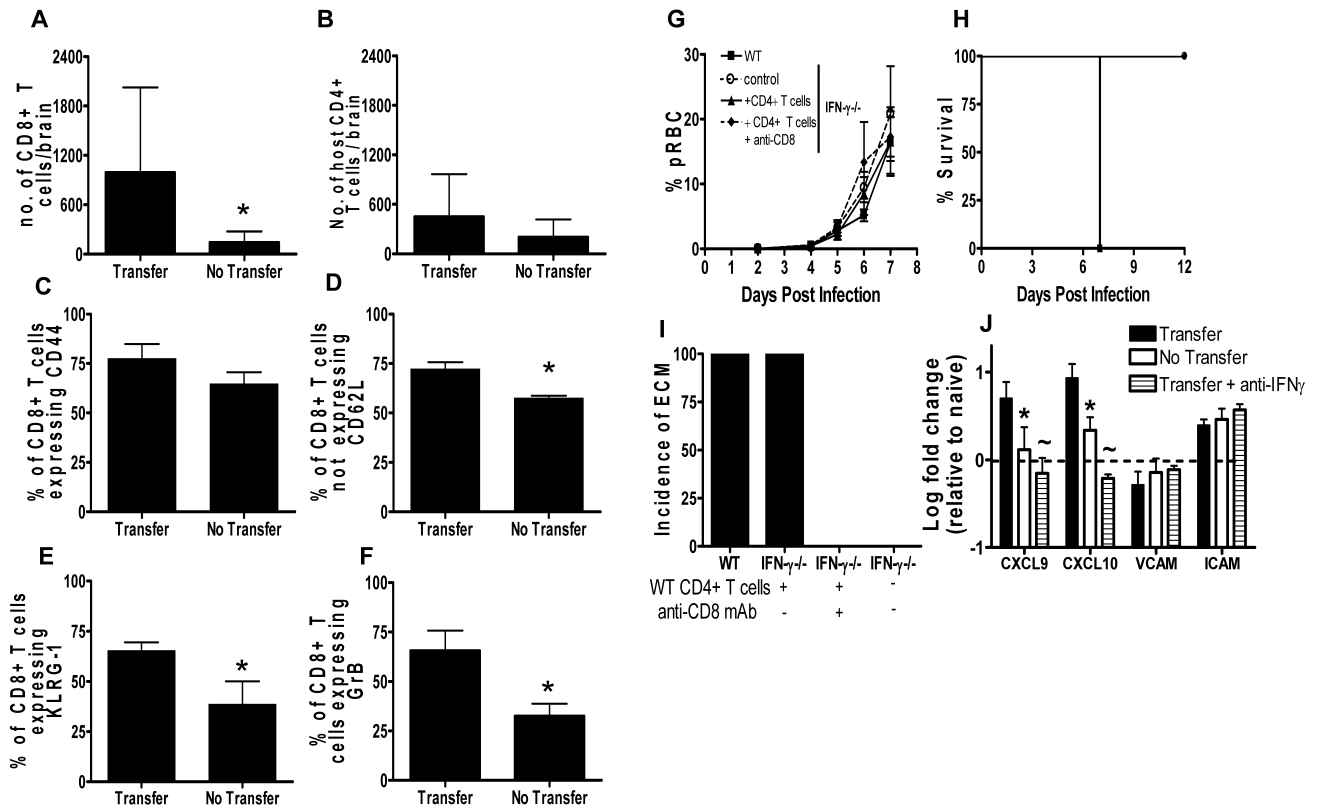
Figure 7. Adoptive transfer of infection-derived IFN-γ producing CD4^{+} T cells promotes ECM in IFN-γ^{−/−} mice by enhancing host CD8^{+} T cell responses within the brain

CD4^{+} T cells were purified from CD45.1^{+}C57BL/6 mice on day 5 of *P. berghei* ANKA infection (10[4] pRBC i.v.) and were adoptively transferred (i.v.) into recipient CD45.2[+]IFN-γ^{−/−} mice one day prior to infection with *P. berghei* ANKA (10[4] pRBC i.v.). A secondary adoptive transfer (i.v.) of day-5 infection derived CD45.1^{+}C57BL/6 CD4^{+} T cells into recipient IFN-γ^{−/−} mice was performed on day 5 of infection. (A, B) The number of host (A) CD8^{+} T cells and (B) CD4^{+} T cells within the brain. (C-E) The frequencies of host CD8^{+} T cells in the brains of IFN-γ^{−/−} mice that received IFN-γ competent CD4^{+} T cells (Transfer) and control infected IFN-γ^{−/−} mice (No Transfer) that were (C) CD44^{+}, (D) CD62L^{low}, (E) KLRG-1^{+} and (F) GrB^{+} on day 7 of infection. (G-J) Recipient mice were injected i.p. with 250μg anti-CD8 on day −2, 0, 2, 4 and 6 of infection. Control recipients of CD4^{+} T cells were injected i.p. with PBS. The course of infection was monitored by following (G) peripheral parasitaemia and (H) survival. (I) The incidence of ECM was calculated. (J) The expression level of CXCL9, CXCL10, ICAM-1 and VCAM-1 in the brains of IFN-γ^{−/−} mice that received WT CD4^{+} T cells compared to the level in infected IFN-γ^{−/−} control mice that did not receive WT CD4^{+} T cells was calculated relative to the level of expression in naive brains by real time PCR (Taqman) on day 6 or 7 of infection, when the recipients of CD4^{+} T cells developed ECM. The results are the mean +/− SD of the group with 3-4 mice per group. The results are representative of 2-3 separate experiments. * P<0.05 between infected IFN-γ^{−/−} recipients of WT cells vs infected IFN-γ^{−/−} controls
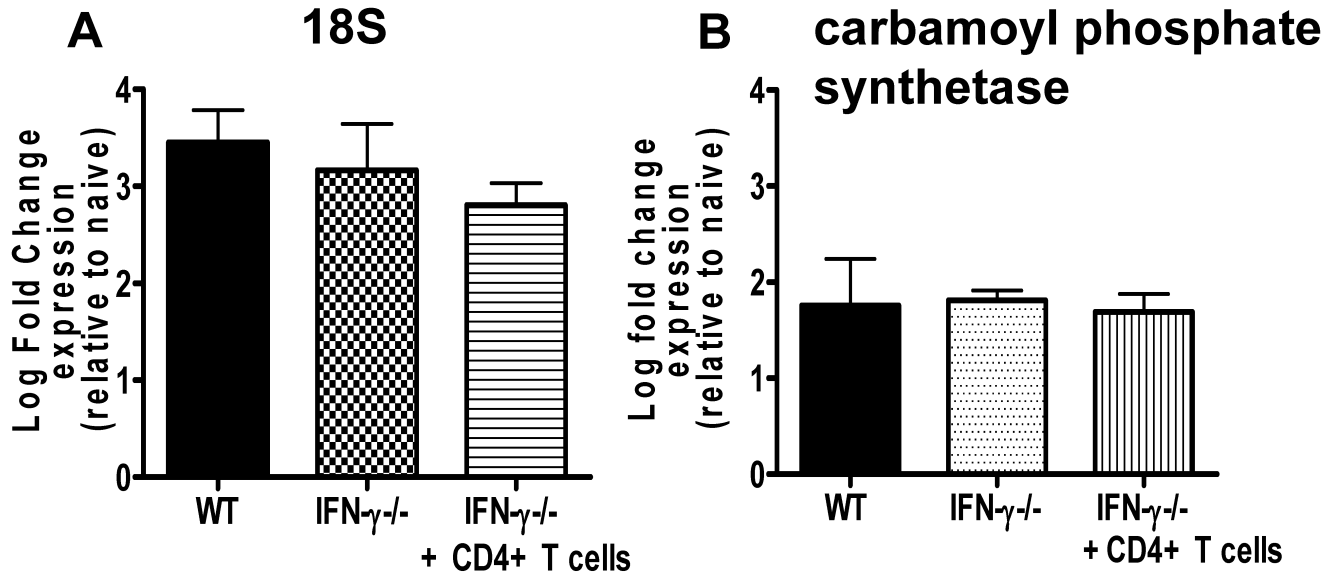
Figure 8. Adoptive transfer of infection-derived IFN-γ producing CD4⁺ T cells does not affect parasite accumulation within the brain during *P. berghei* ANKA infection

CD4⁺ T cells were purified from C57BL/6 mice on day 5 of *P. berghei* ANKA infection (10^4 pRBC i.v.) and were adoptively transferred (i.v.) into recipient IFN-$\gamma^{-/-}$ mice one day prior to infection with *P. berghei* ANKA (10^4 pRBC i.v.). A secondary adoptive transfer (i.v.) of day 5 infection-derived C57BL/6 CD4⁺ T cells into recipient IFN-$\gamma^{-/-}$ mice was performed on day 5 of infection. (A, B) The expression level of parasite (A) 18S and (B) carbamoyl phosphate synthetase genes in the perfused brains were determined on day 7 of infection by real-time PCR (Sybergreen). Results are expressed as the log fold change relative to the level in the brains of naive mice. The results are the mean +/− SD of the group with 3-5 mice per group. The results are representative of 3 separate experiments.

Table I

The incidence of ECM and severity of infection in IFN-γ$^{-/-}$ mice following adoptive transfer of naive and infection-derived IFN-γ competent leukocytes.

Population of cells transferred*	Day of transfer	Incidence of any clinical signs (%) #	Mean maximum clinical score#,†	Incidence of clinical signs 4-5 (%) #	Total number of mice
Naive Splenocytes	D-1	100	2.5	0	8
Naive RAG-1$^{-/-}$ splenocytes	D-1	0	1	0	6
Naive αβ$^+$ T cells	D-1	100	3.1	9	11
Naive CD4$^+$ T cells	D-1	100	2.8	0	8
Naive CD8$^+$ T cells	D-1	0	1	0	8
I-D αβ$^+$ T cells	D-1	100	3.25	25	8
I-D αβ$^+$ T cells	D+5	100	3.75	50	8
I-D αβ$^+$ T cells	D-1 + D5	100	4	100	10
I-D RAG-1$^{-/-}$ splenocytes	D-1	0	1	0	6
I-D CD4$^+$ T cells	D-1 + D5	100	4.6	100	17
I-D CD4$^+$ T cells	D+5	100	3.0	0	7
I-D CD8$^+$ T cells	D-1 + D5	0	1	0	14

All experiments performed 2-5 times with 3-5 mice per group.

*
WT C57/BL6 donors unless stated

I-D Cells derived from infected (Day 5) donors

#
During ECM window period of infection (D6-D11)

†
Grading system described in materials and methods